Spectrum-Based Online Estimation of IQ Imbalance for Near Field Radar Distance Sensors

Florian Liebgott*, Marvin Jandt*†, Mark Eberspächer*, Annika Liebgott† and Bin Yang†
*Balluff GmbH, Neuhausen a.d.F., Germany
†Institute of Signal Processing and System Theory, University of Stuttgart, Germany
Email: florian.liebgott@balluff.de

***Abstract*—A mismatch of the in-phase (I) and quadrature (Q) signal path of a direct-conversion receiver results in IQ imbalance, which distorts the demodulated signal. However, if the imbalance parameters can be estimated, the influence of the IQ imbalance can be compensated. We propose a novel method to estimate the parameters during normal operation of a stepped frequency continuous wave (SFCW) radar distance sensor without the need for a pilot signal. To estimate the imbalance parameters, we exploit the structure of the spectrum of the demodulated signal. Evaluating our method on real sensor data shows superior results especially for very short distances.**

***Index Terms*—radar sensor, IQ imbalance, near field**

I. Introduction

Quadrature receivers often suffer from IQ imbalance caused by a mismatch of the in-phase (I) and quadrature (Q) signal path, resulting in a distorted demodulated signal. For radar sensors, this leads to a reduction of accuracy and should therefore be compensated.

A frequently used method for IQ imbalance compensation is the utilization of known pilot signals [1]. The parameters of the IQ imbalance can be determined from the deviation of the demodulated signals from the known pilot signal. Another approach is to use the circularity of the received signal to correct the IQ imbalance without pilot signals [2], [3].

For radar distance sensors, IQ imbalance estimation often uses a pilot signal, which is e.g. generated with a phase shifter [4] or a target performing a sinusoidal motion [5], [6].

Due to aging of the hardware or temperature changes, IQ imbalance may change over time. To avoid a degradation of accuracy caused by changed IQ imbalance parameters, the parameters could be estimated online. However, this is not feasible using pilot signals. As the IQ imbalance transforms a received circular signal in the complex (I, Q) domain into an ellipse, one approach for online estimation is to fit an ellipse to the demodulated data and estimate the IQ imbalance from the ellipse's parameters [5], [7].

The mentioned approaches are used with radar sensors operating in the far field only. We, in contrast, investigate the online IQ imbalance compensation of a stepped frequency continuous wave (SFCW) radar distance sensor for a near distances range of up to zero mm, i.e. a sensor operating in or close to the near field. For such sensors, the aforementioned approaches are not feasible. In the near field, the attenuation of the received signal strongly depends on the distance d of the target to the sensor. The received signal thus describes a spiral instead of a circle, as shown in Fig. 1. Estimating the IQ imbalance by ellipse fitting or with circularity-based approaches is therefore not suitable for near field applications.

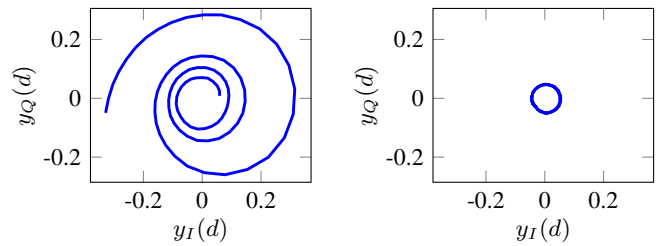

Fig. 1. Near field signal (left) with attenuation clearly depending on distance d and far field signal (right) with nearly distance independent attenuation.

We propose an alternative approach for online IQ imbalance estimation based on the spectrum of the received signal. IQ imbalance results in the spectrum of the received signal being superimposed with a mirrored image of the spectrum. We propose a novel approach to estimate the IQ imbalance from the ratio of the desired signal's spectrum and the image spectrum by disaggregating the spectrum into these two components. Our goal is to estimate the IQ imbalance parameters during the normal operation of the sensor.

II. IQ Imbalance

In a quadrature receiver, the received signal is first multiplied with the local oscillator (LO) signal, whose frequency matches the carrier frequency. Then it is amplified and filtered with a low-pass filter before being digitized. If a quadrature design is used, the receiver has two paths, the in-phase (I) path and the quadrature (Q) path.

The received signal $r(t)$ with carrier frequency ω_0 containing the I signal $x_I(t)$ and the Q signal $x_Q(t)$ is given as

$$r(t) = x_I(t)\cos(\omega_0 t) + x_Q(t)\sin(\omega_0 t). \tag{1}$$

This signal is multiplied with the LO signals $s_I(t) = \cos(\omega_0 t)$ and $s_Q(t) = \sin(\omega_0 t)$ of the I and Q path, respectively. The multiplication produces the signals

$$\begin{aligned} u_I(t) &= r(t)s_I(t) && (2)\\ &= x_I(t)\cos^2(\omega_0 t) + x_Q(t)\sin(\omega_0 t)\cos(\omega_0 t) && (3)\\ &= \frac{x_I(t)}{2}\left(1+\cos(2\omega_0 t)\right) + \frac{x_Q(t)}{2}\sin(2\omega_0 t) && (4) \end{aligned}$$

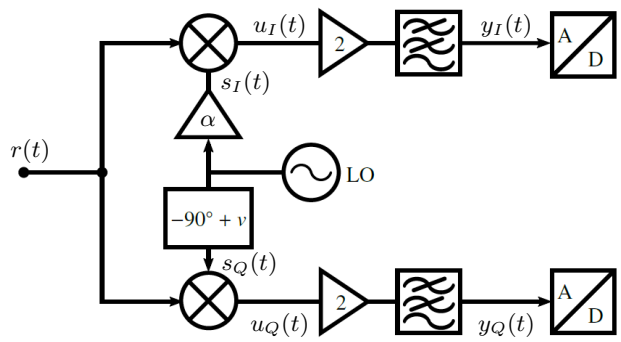

Fig. 2. Block diagram of a direct-conversion receiver with IQ imbalance.

and

$$u_Q(t) = r(t)s_Q(t) \tag{5}$$
$$= x_I(t)\cos(\omega_0 t)\sin(\omega_0 t) + x_Q(t)\sin^2(\omega_0 t) \tag{6}$$
$$= \frac{x_I(t)}{2}\sin(2\omega_0 t) + \frac{x_Q(t)}{2}\left(1 - \cos(2\omega_0 t)\right). \tag{7}$$

Amplifying $u_I(t)$ and $u_Q(t)$ by a factor of two and low-pass filtering them results in the desired demodulated signals

$$y_I(t) = x_I(t) \quad \text{and} \tag{8a}$$
$$y_Q(t) = x_Q(t). \tag{8b}$$

A mismatch between the I and Q path, caused for example by a deviation of the phase shift of the LO signal or by a difference in the amplification, results in IQ imbalance. The imbalance consists of a phase and a gain imbalance. Both can be modeled by modifying the LO signals $s_I(t)$ and $s_Q(t)$ to include the gain imbalance α and the phase imbalance ν. Without loss of generality, we assume

$$s_I(t) = \alpha\cos(\omega_0 t) \quad \text{and} \tag{9a}$$
$$s_Q(t) = \sin(\omega_0 t + \nu). \tag{9b}$$

Fig. 2 shows the block diagram of a quadrature receiver with IQ imbalance modeled this way.

After demodulation, the resulting I and Q signals are

$$y_I(t) = \alpha x_I(t) \quad \text{and} \tag{10a}$$
$$y_Q(t) = x_I(t)\sin(\nu) + x_Q(t)\cos(\nu). \tag{10b}$$

The relationship between the demodulated signals $y_I(t)$ and $y_Q(t)$ and the desired signals $x_I(t)$ and $x_Q(t)$ can also be expressed using a distortion matrix $\mathbf{M}$:

$$\begin{pmatrix} y_I(t) \\ y_Q(t) \end{pmatrix} = \mathbf{M}\begin{pmatrix} x_I(t) \\ x_Q(t) \end{pmatrix}, \quad \mathbf{M} = \begin{pmatrix} \alpha & 0 \\ \sin(\nu) & \cos(\nu) \end{pmatrix} \tag{11}$$

To correct the IQ imbalance, we rearrange (11) to calculate the desired signals

$$\begin{pmatrix} x_I(t) \\ x_Q(t) \end{pmatrix} = \mathbf{M}^{-1}\begin{pmatrix} y_I(t) \\ y_Q(t) \end{pmatrix} \tag{12}$$

with the inversed distortion matrix

$$\mathbf{M}^{-1} = \begin{pmatrix} \frac{1}{\alpha} & 0 \\ -\frac{\tan(\nu)}{\alpha} & \frac{1}{\cos(\nu)} \end{pmatrix}. \tag{13}$$

Consequently, if we can estimate the phase imbalance ν and the gain imbalance α, we can easily correct the IQ imbalance.

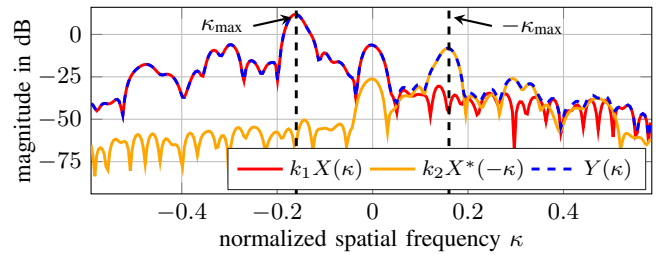

Fig. 3. Magnitude of the Fourier transform $Y(\kappa)$ and its components $k_1X(\kappa)$ and $k_2X^*(-\kappa)$ for $\alpha = 0.99$ and $\nu = 1°$.

III. IQ Imbalance Estimation

In contrast to quadrature receivers in use for communications, the received signal of an SFCW distance radar does not depend on the time t but on the distance d of a target to the sensor. The complex demodulated signal in the spatial domain for a fixed carrier frequency is thus

$$y(d) = y_I(d) + \mathrm{j}y_Q(d). \tag{14}$$

The desired signals $x_I(d)$ and $x_Q(d)$ can be expressed as real and imaginary part of $x(d) = x_I(d) + \mathrm{j}x_Q(d)$:

$$x_I(d) = \mathrm{Re}\{x(d)\} = \frac{x(d) + x^*(d)}{2} \quad \text{and} \tag{15a}$$
$$x_Q(d) = \mathrm{Im}\{x(d)\} = \frac{x(d) - x^*(d)}{2\mathrm{j}}. \tag{15b}$$

Inserting this into (11) and simplifying leads to

$$y(d) = \frac{\alpha + \mathrm{e}^{\mathrm{j}\nu}}{2}x(d) + \frac{\alpha - \mathrm{e}^{-\mathrm{j}\nu}}{2}x^*(d). \tag{16}$$

By setting

$$k_1 = \frac{\alpha + \mathrm{e}^{\mathrm{j}\nu}}{2} \quad \text{and} \tag{17a}$$
$$k_2 = \frac{\alpha - \mathrm{e}^{-\mathrm{j}\nu}}{2}, \tag{17b}$$

we can write (16) as

$$y(d) = k_1 x(d) + k_2 x^*(d). \tag{18}$$

Using the Fourier transform, we can express the demodulated signal in the spatial frequency domain as

$$Y(\kappa) = \mathcal{F}\{y(d)\} = k_1 X(\kappa) + k_2 X^*(-\kappa). \tag{19}$$

The resulting signal $Y(\kappa)$ thus consists of the desired signal $X(\kappa)$, which is superimposed with a scaled, mirrored and complex conjugated copy of itself. In an ideal receiver, this image would be completely suppressed due to $k_2 = 0$.

Fig. 3 shows the magnitude of the resulting signal $Y(\kappa)$ and its components. As a distance increase of half the wavelength corresponds to one complete rotation in the complex (I, Q) plane, the maximum of the spectrum is at the normalized spatial frequency $\kappa_{\max}$ corresponding to half the wavelength. At the mirrored spatial frequency $-\kappa_{\max}$, the maximum of the image occurs. The spectrum at those frequencies is given as

$$Y(\kappa_{\max}) = k_1 X(\kappa_{\max}) + k_2 X^*(-\kappa_{\max}) \quad \text{and} \tag{20a}$$
$$Y(-\kappa_{\max}) = k_1 X(-\kappa_{\max}) + k_2 X^*(\kappa_{\max}). \tag{20b}$$

If we assume that there is only one target present in the measuring range, the signal is approximately zero at the mirrored frequency $-\kappa_{\text{max}}$, which results in

$$Y(\kappa_{\text{max}}) \approx k_1 X(\kappa_{\text{max}}) \quad \text{and} \tag{21a}$$

$$Y(-\kappa_{\text{max}}) \approx k_2 X^*(\kappa_{\text{max}}). \tag{21b}$$

Consequently, only the desired signal contributes to the spectrum at the frequency κ_{max} and the spectrum at the mirror frequency $-\kappa_{\text{max}}$ is only influenced by the image. Defining

$$K = \frac{Y(-\kappa_{\text{max}})}{Y^*(\kappa_{\text{max}})}, \tag{22}$$

we get

$$K \approx \frac{k_2}{k_1^*} = \frac{\alpha - \mathrm{e}^{-\mathrm{j}\nu}}{\alpha + \mathrm{e}^{-\mathrm{j}\nu}}, \tag{23}$$

which can be used to estimate the imbalance parameters as

$$\hat{\alpha} = \left|\frac{1+K}{1-K}\right| \quad \text{and} \tag{24}$$

$$\hat{\nu} = \arg\left(\frac{1+K}{1-K}\right). \tag{25}$$

IV. Evaluation

We evaluated the performance of our proposed "image" method in several experiments using real data measured with an SFCW radar distance sensor. The measurements were carried out with carrier frequencies between 24 GHz and 26 GHz. We compared the results of our image method to a method for offline IQ imbalance estimation using a pilot signal and to the ellipse method proposed in [5].

An often used quantity to assess a receiver is the signal-to-image ratio (SIR). It is defined as the ratio of the spectral power of the desired signal to that of the image, that is

$$\text{SIR} = \frac{|k_1|^2}{|k_2|^2} = \frac{1+\alpha^2+2\alpha\cos(\nu)}{1+\alpha^2-2\alpha\cos(\nu)}. \tag{26}$$

A. Offline IQ Imbalance Estimation with Pilot Signal

First, we used the pilot signal utilized for the offline estimation to evaluate our proposed method. The pilot signal is a circular signal without attenuation equidistantly sampled over a distance of twice the wavelength, which equals four rotations in the (I, Q) plane. Our image approach as well as the ellipse method yield very similar results to the pilot method, see Fig. 4. For both the estimated gain and phase imbalance, the differences between the methods are very small across all investigated carrier frequencies. For all methods, the corrected resulting signal is a circle. Consequently, our proposed method is suitable for offline IQ imbalance correction.

B. Online IQ Imbalance Estimation

To evaluate the online estimation capabilities of our approach, we measured the received signal for different target positions. We moved the target from a distance of zero to 190 mm with a spatial resolution of 0.1 mm.

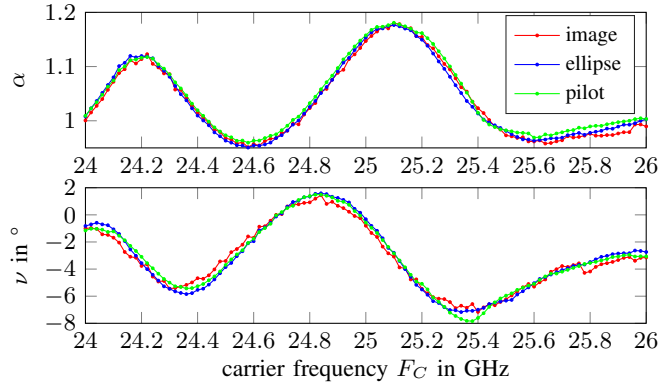

Fig. 4. Gain and phase imbalance α and ν, respectively, estimated from a pilot signal.

1) Mean Target Distance: In order to evaluate the influence of the target distance during the IQ imbalance estimation, we used intervals with a length of 20 mm each as input for the imbalance estimation. The results show that the success of the estimation methods strongly depends on the target distance. For short distances, the image method is very close to the results of the pilot method, while the ellipse method does not work reliably. Fig. 5 shows the gain and phase imbalance estimated from measurements between zero and 20 mm. The imbalance parameters estimated with the ellipse method show a strong oscillation over the carrier frequencies and deviate considerably from the pilot method. On the other hand, the difference between the parameters estimated with the image and the pilot method is slightly more noticeable than with the pilot signal, but remains small.

The result of using these estimated imbalance parameters to correct the measurement is depicted in Fig. 6 and Fig. 7. Both in the spatial and the spatial frequency domain, the difference between the ellipse method and the other methods is clearly visible. It manifests in a visible deformation of the spiral in the spatial domain and the amplification of the image signal in the spatial frequency domain. Our proposed method, in contrast, reduces the image signal even more than the pilot method.

The ellipse method's poor performance for short distances is not surprising, as the signal resembles a spiral instead of an ellipse. For larger distances, the turns of the spiral are closer together and thus more similar to a circle or an ellipse.

To evaluate the methods, we calculated the mean SIR over all carrier frequencies. The uncorrected signal exhibits a mean SIR of 28.8 dB. Using the parameters estimated with the pilot method, the mean SIR can be increased to 42.9 dB. Our proposed method further increases the mean SIR by over 10 dB to 53.7 dB. As already expected from Fig. 7, the mean SIR of the ellipse method (18.5 dB) is significantly lower than the one of the uncorrected signal.

Fig. 8 shows the mean SIR of our proposed method, the ellipse and pilot method and the uncorrected signal for different target distances. The depicted distances are the mean distance of each interval of length 20 mm used for the estimation of the IQ parameters. The SIR achieved with our method is above the pilot SIR for almost all distance intervals. It achieves

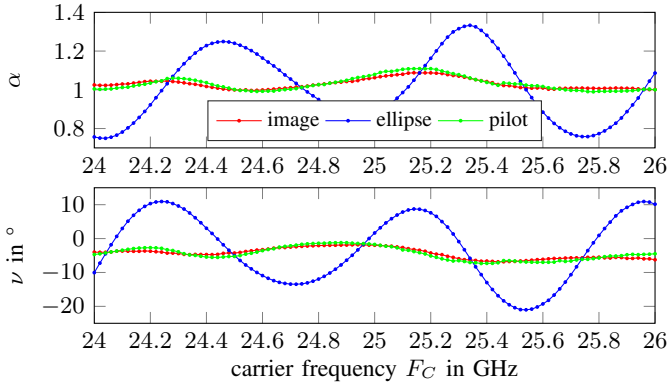

Fig. 5. Gain and phase imbalance α and ν, respectively, estimated from target distances between 0 mm and 20 mm with a spatial resolution of 0.1 mm.

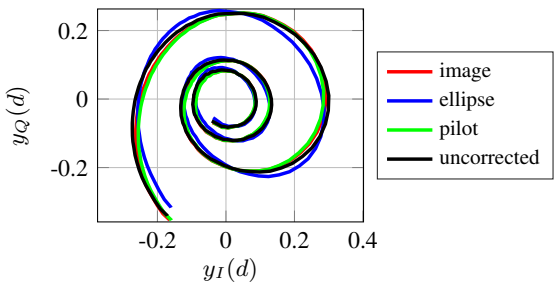

Fig. 6. Demodulated signal $y(d)$ for distances between 0 and 20 mm with $F_C = 24.28$ GHz and the IQ corrected versions of the signal.

its highest SIRs for shorter distances and decreases slightly for larger distances. In contrast, the ellipse method performs poorly for smaller distances and stabilizes above 70 mm, but on a lower level than both other methods.

2) Number of Samples With a Fixed Spatial Resolution: We evaluated the influence of the number of samples used for the parameter estimation, when the spatial resolution remains unchanged. In the previous experiment, we used 200 samples with a sample distance of 0.1 mm to estimate the parameters. We now estimate the parameters using 50, 100, 150, 200 and 400 samples with the same spatial resolution. Fig. 9 shows the mean SIRs for the signals corrected using these estimates. For the image method, using less than 150 samples for parameter estimation leads to lower SIRs than the uncorrected signal. The ellipse method, in contrast, performs equally well for all examined cases, therefore outperforming the otherwise

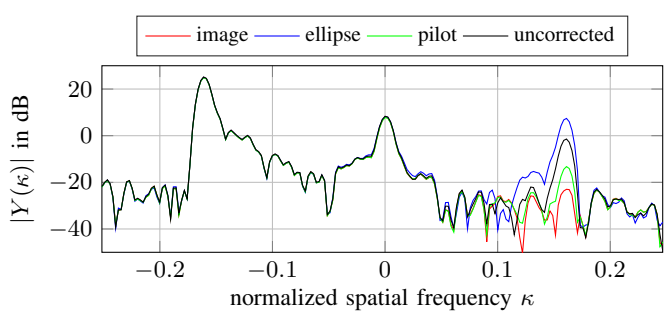

Fig. 7. Magnitude of the Fourier transform $Y(\kappa)$ of the demodulated signal for distances between 0 and 20 mm with $F_C = 24.28$ GHz and the IQ corrected versions of the signal.

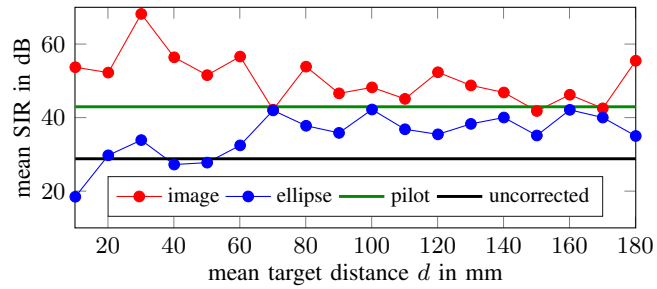

Fig. 8. Mean SIR over the middle distance of each interval with a width of 20 mm used for estimation of the correction parameters.

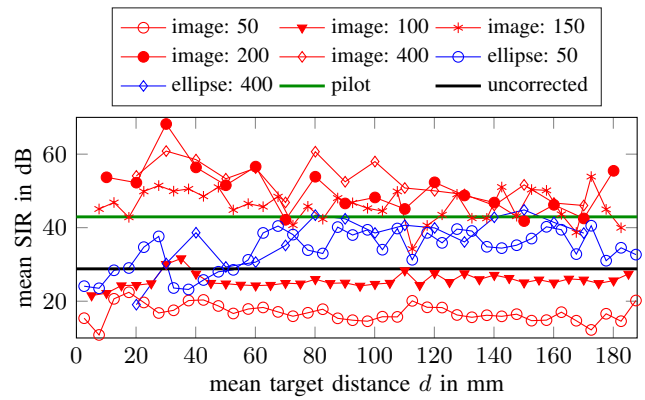

Fig. 9. Mean SIR with different number of samples used for the parameter estimation over the mean distance of the interval used for estimation of the correction parameters.

superior image method significantly for less than 150. For 50 samples with a spacing of 0.1 mm, the samples form eight tenths of an ellipse, which is enough to estimate the ellipse parameters. Further investigations showed degrading performance of the ellipse method for fewer samples than 50.

3) Spatial Resolution: In contrast to the previous section, we now change the spatial resolution while keeping the distance interval used for estimation at 20 mm. The SIR resulting from correction parameters estimated at different spatial resolutions is shown in Fig. 10. With a sample distance of 2 mm, which results in only ten samples being used for estimation, the image method yields an SIR mostly below the SIR of the uncorrected signal. The performance increases significantly with the spatial resolution. For target distances below 70 mm, it outperforms the pilot method even for a sample distance of $\frac{2}{3}$ mm. The ellipse method also performs unsatisfactorily for a sample distance of 2 mm and achieves good results comparable to Fig. 8 for higher spatial resolutions.

To better understand the influence of spatial resolution, we evaluated the SIR for different spatial resolutions with a fixed number of samples. In contrast to the previous experiment, the distance interval covered by the samples used for estimation is not fixed anymore. Fig. 11 shows the results for different spatial resolutions using 65 samples for the estimation.

In this case, the SIR of the image method for a sample distance of 0.1 mm is worse than the SIR of the uncorrected signal. This is in line with our previous finding that given this spatial resolution, we need at least 150 samples to get

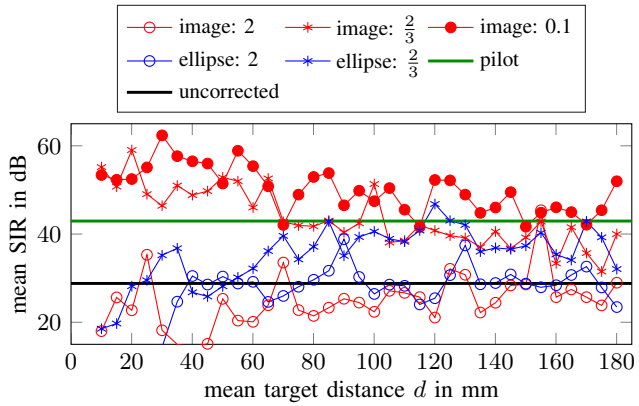

Fig. 10. Mean SIR for different sample distances used for the parameter estimation over the middle distance of the 20 mm interval used for estimation of the correction parameters.

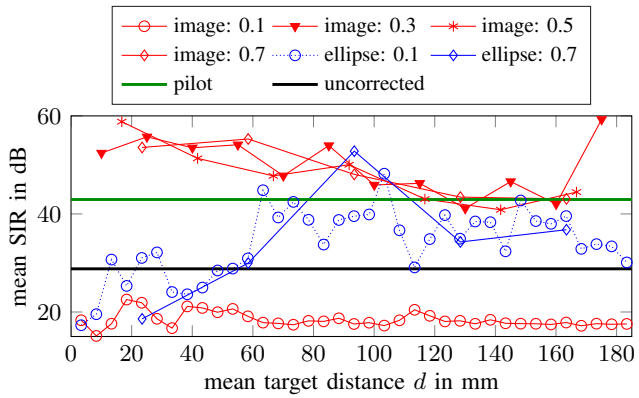

Fig. 11. Mean SIR for different spatial resolutions used for the parameter estimation over the middle distance of the 65 samples long interval used for estimation of the correction parameters.

good results. For sample distances of 0.3 mm and above, the image method performs comparably to 200 samples with a sample distance of 0.1 mm, but with reduced fluctuations. This implies, that in order for the image method to produce meaningful results, the samples used for estimation need to cover an interval of at least one to 1.5 times the wavelength, which corresponds to two to three rotations in the (I, Q) plane.

The ellipse method performs comparably well for all spatial resolutions, but exhibits stronger fluctuations in comparison to previous experiments.

C. Non-Equidistantly Sampled Data

In the previous experiments, we assumed the data to be sampled equidistantly. This is possible, if the sensor is used to measure targets with a uniform movement. However, this does not necessarily correspond to real-world applications. We therefore investigated the methods' performance, if the data is not sampled equidistantly. For the ellipse method, this has no influence on the results. The image method, however, requires equidistantly sampled data to perform the discrete Fourier transform (DFT). We chose to use cubic interpolation to get uniformly distributed samples. As the signal is smooth, the interpolation works well, provided that there are enough samples per rotation. Our experiments showed that the interpolation performs very well, if the maximum distance between two samples is not larger than one tenth of the wavelength, which corresponds to one fifth rotation in the (I, Q) plane.

D. Noisy Distance Information

While the ellipse method relies solely on the shape the samples form in the (I, Q) plane, the image method depends on the correct distance information for each sample. As the online IQ imbalance estimation is to be carried out during normal operation, the distance information has to come from the sensor itself. This information is influenced by several factors, amongst others how well the IQ imbalance is currently compensated. We thus investigated the influence of noisy distance information on the image method.

We found that the critical factor is whether the noise leads to samples not being in the same order as their distance information. Assuming a normally distributed distance noise, if the standard deviation of the noise is smaller than a third of the sample distance, less than 1 % of neighboring samples are swapped and the SIR is slightly degraded. For a standard deviation of one fourth of the sample distance, this decreases to less than 0.05 %. In contrast, standard deviations of more than half the sample distance lead to unsatisfactory results.

V. Conclusions

We presented a method for online estimation of IQ imbalance from the spectrum without the use of pilot signals. We evaluated the method using an SFCW radar distance sensor and compared it to the ellipse method. When used on a pilot signal, our proposed image method performed as well as an offline estimation using pilot signals. For online correction, it outperformed both the ellipse and pilot method, if the samples are distributed over an interval of at least one to 1.5 times the wavelength and the distance information is not too noisy.

Using our method, online estimation of the IQ imbalance of an SFCW radar distance sensor during operation in or close to the near field is feasible.

References

[1] F. E. Churchill, G. W. Ogar, and B. J. Thompson, "The correction of I and Q errors in a coherent processor," *IEEE Transactions on Aerospace and Electronic Systems*, vol. 17, pp. 131–137, 1981.

[2] L. Anttila, M. Valkama, and M. Renfors, "Blind compensation of frequency-selective I/Q imbalances in quadrature radio receivers: Circularity-based approach," in *IEEE International Conf. on Acoustics, Speech and Signal Processing - ICASSP '07*, 2007, pp. III–245–III–248.

[3] M. Ulrich and B. Yang, "IQ and array calibration for FMCW radar," in *2017 18th International Radar Symposium (IRS)*, 2017, pp. 1–10.

[4] B.-K. Park, S. Yamada, and V. Lubecke, "Measurement method for imbalance factors in direct-conversion quadrature radar systems," *IEEE Microwave and Wireless Comp. Letters*, vol. 17, no. 5, pp. 403–405, 2007.

[5] A. Singh, X. Gao, E. Yavari, M. Zakrzewski, X. H. Cao, V. M. Lubecke, and O. Boric-Lubecke, "Data-based quadrature imbalance compensation for a CW doppler radar system," *IEEE Transactions on Microwave Theory and Techniques*, vol. 61, pp. 1718–1724, 2013.

[6] M. Pieraccini, N. Donati, and F. Papi, "I-Q imbalance correction of microwave displacement sensors," *Electronics Letters*, vol. 51, no. 13, pp. 1021–1023, 2015.

[7] S. H. Chang, H. S. Chung, and K. Kim, "Impact of quadrature imbalance in optical coherent QPSK receiver," *IEEE Photonics Technology Letters*, vol. 21, pp. 709–711, 2009.